ELSEVIER

Physica C 261 (1996) 56–64

PHYSICA C

The origins of high values of the critical current density in the $Bi_2Sr_2Ca_{n-1}Cu_nO_x$ system: high-T_c superconducting pathways at low angle tilt boundaries

Y. Yan [a,*], J.E. Evetts [a,b], B. Soylu [b], W.M. Stobbs [b]

[a] IRC in Superconductivity, Cambridge University, Madingley Road, Cambridge CB3 0HE, UK
[b] Department of Materials Science and Metallurgy, Cambridge University, Pembroke St., Cambridge CB2 3QZ, UK

Received 6 October 1995; revised manuscript received 19 February 1996

Abstract

Low angle tilt boundaries in melt processed samples from the $Bi_2Sr_2Ca_{n-1}Cu_nO_x$ system exhibit compositionally modulated faceting. Although we see local regions of the low-T_c (20 K) (2201) phase at such boundaries which would be highly resistive at liquid nitrogen temperatures, there are also "pathways" crossing the boundary plane made up of the high-T_c (2212) and (2223) phases. The characteristics of such low angle tilt grain boundary structures can therefore be modelled to provide a general insight into the correlation between high critical current densities and low texture breadths.

1. Introduction

It is generally accepted that the critical current density of high temperature superconductors is strongly affected by the nature and form of the grain boundaries. For the $Bi_2Sr_2Ca_{n-1}Cu_nO_x$ system the critical current density, J_c, can be particularly high for textured samples that are well aligned with the *c* axis perpendicular to the direction of current flow. Uno et al. [1] demonstrated that, the worse the *c* axis alignment, the more rapidly J_c falls off as a function of applied magnetic field. The high J_c values of well aligned $Bi_2Sr_2Ca_{n-1}Cu_nO_x$ tapes were explained by Bulaevskii et al. [2] on their "brick wall" model. According to this model the current flows between grains in the *c* direction across the (001) twist boundaries [3–6] that are predominant in such tapes, and a weak link is expected to be formed at non basal plane boundaries between abutting grains. However it is not clear why such a model can explain high J_c values when the *c* axes of the grains are not accurately aligned. The persistence of J_c to high magnetic fields at low temperatures indicates that these materials are not coupled by weak links. Hensel et al. [7] have invoked a "railway switch" model for J_c in which the current is channelled between grains by low angle tilt boundaries. The evidence for their model is inferred indirectly, for example, from the low tendency to etching for such boundaries [7]. The J_c data presented indicate that their model is probably more appropriate than the "brick wall" model for these materials.

Here we discuss the origins of high J_c values in the $Bi_2Sr_2Ca_{n-1}Cu_nO_x$ system in the presence of low angle tilt misorientations. Characteristic low angle tilt boundaries have been described for the mate-

---

[*] Corresponding author. Fax: +44 223 337074.

PII S0921-4534(96)00179-7

rial [3,4,8,9]. These boundaries are apparently present for specimens with a high J_c [e.g. 1,7,10]. In the $YBa_2Cu_3O_{7-\delta}$ system, grain boundary structures are strongly affected by impurity segregation [11,12] or variations in local stoichiometry [13,14], and thus tend to act as weak links in the superconducting state. Although grain boundaries in the $Bi_2Sr_2Ca_{n-1}Cu_nO_x$ system also exhibit changes in local stoichiometry [3,8,9], the form of the associated local structural changes for low angle tilt boundaries (with or without associated twist components) is completely different to that observed in the $YBa_2Cu_3O_{7-\delta}$ system. It is these specific characteristics of the grain boundary structures in $Bi_2Sr_2Ca_{n-1}Cu_nO_x$, in particular those associated with low angle tilts, which we suggest allow the current flow required by the "railway switch" model for low angle tilt boundaries.

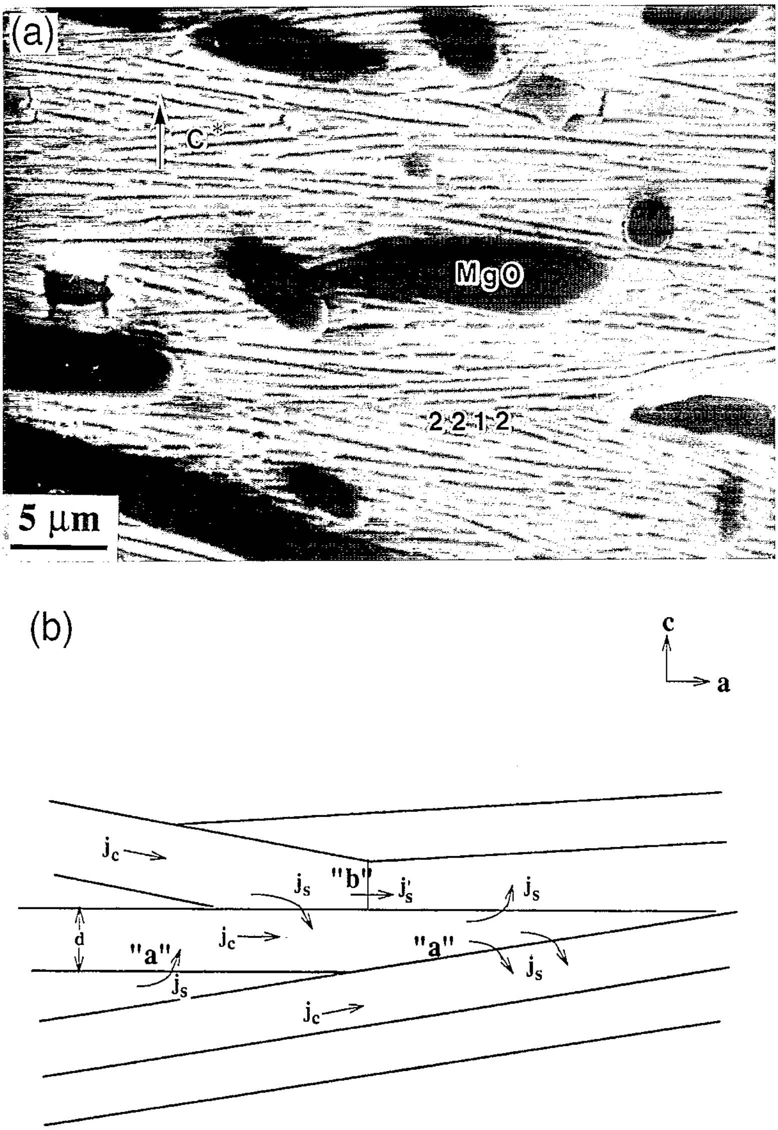

Fig. 1. a) SEM micrograph showing a cross-sectional area of a textured CRT (2212) specimen. b) A schematic of the characteristic grain boundary structure in a textured (2212) sample in which two different kinds of path are labelled: "a" across the low habit angle boundaries (the boundary plane being nearly parallel to the *a*–*b* planes) and "b" across the high habit angle boundaries (the boundary plane being nearly perpendicular to the *a*–*b* planes). The current densities along the *a*–*b* plane within grains and across the grain boundaries are labelled by j_c and j_s.

2. Grain boundary structures in $Bi_2Sr_2Ca_{n-1}Cu_nO_x$

The different phases in the $Bi_2Sr_2Ca_{n-1}Cu_nO_x$ system are closely related: they all contain BiO double layers sandwiching perovskite-type units containing Sr, Ca, Cu and O, and are characterised by the number of CuO_2 layers, n, oriented parallel to the (001) plane in the half unit cell [15–17]. The phases $Bi_2Sr_2CuO_x$ ($c = 2.46$ nm), $Bi_2Sr_2Ca_1Cu_2O_x$ ($c = 3.09$ nm), $Bi_2Sr_2Ca_2Cu_3O_x$ ($c = 3.7$ nm) for $n = 1$, 2 and 3 respectively are termed (2201), (2212) and (2223) for brevity and have critical temperatures, T_c, of about 20, 80, and 110 K respectively. The majority phase in our samples was (2212) [9,18]. Inert MgO whiskers were used during processing to

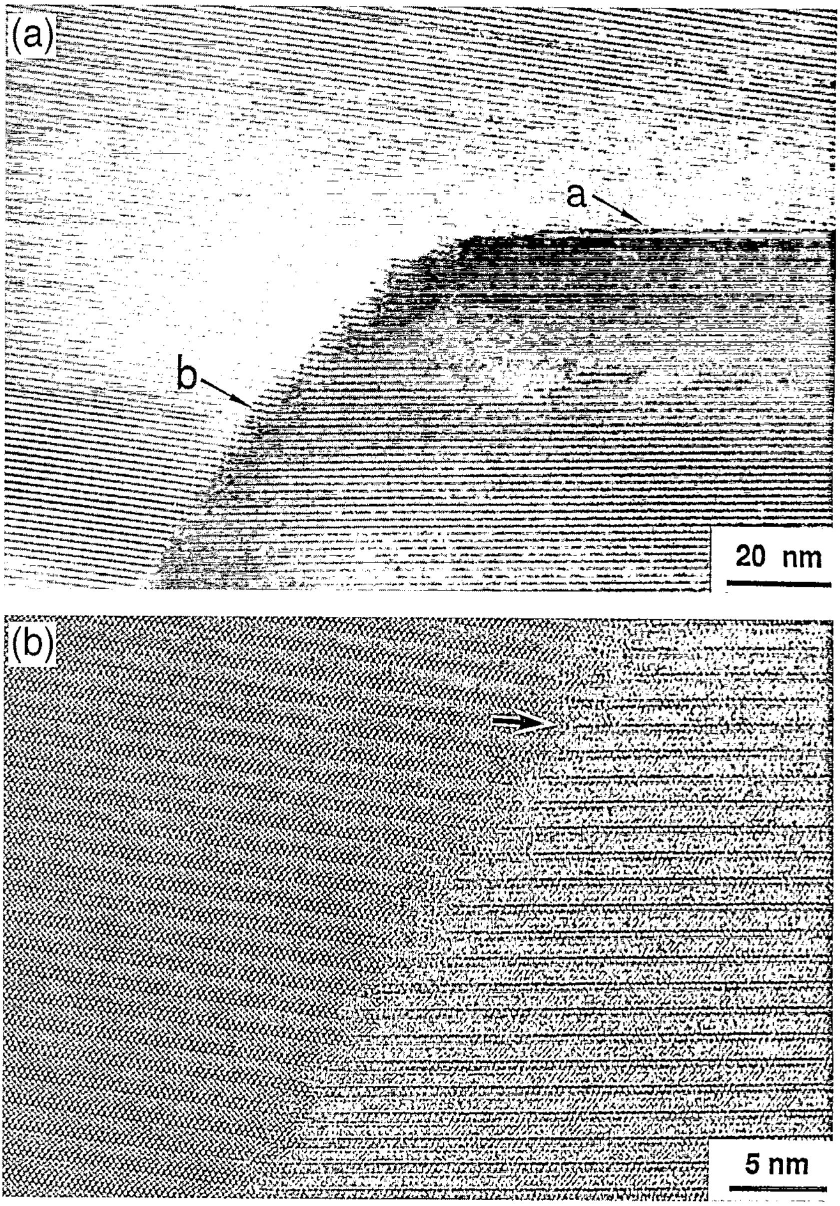

Fig. 2. a) A low magnification image of a grain impinging upon a second grain with an 8° tilt angle of misorientation between the two c axes where the grains are also misoriented by 90° about the c axis with the b axis nearly parallel to the a axis. b) HREM image of the "b" type boundary (marked by "b" in Fig. 2a).

align the superconducting grains and control their morphology by "composite reaction texturing" (CRT) [18]. For an optimised microstructure J_c was in excess of 2×10^4 Acm^{-2} at 4.5 K and 12 T, and 4×10^3 Acm^{-2} at 77 K in zero applied magnetic field. We believe the grain boundary structural data we report here are of equal relevance for other $Bi_2Sr_2Ca_{n-1}Cu_nO_x$ alloys if they are processed to exhibit *c* axis alignment.

Scanning electron microscopy indicates that the melt processed $Bi_2Sr_2CaCu_2O_x$ tends to form grains which are tens of microns wide and just fractions of a micron thick in the *c* direction (see Fig. 1a). These plate-like grains commonly have an aspect ratio of length to thickness greater than 10^2. A schematic of the characteristic grain structure is shown in Fig. 1b. Grains often terminate in low angle wedge like intersections where the a–b planes end (marked "a"), or less frequently in "head-on" boundaries where there can be continuity of the a–b planes from grain to grain (marked "b"). In these $Bi_2Sr_2CaCu_2O_x$ samples the fractional area of type "a" low angle boundaries is far higher than that of type "b".

Fig. 2a shows a low magnification image of one grain impinging upon another at a relative tilt of about 8°, the grains are also twist misoriented by almost precisely 90° about their *c* axes. The habit plane of the boundary changes from type "a" to type "b" in the field of view. In the lower part of Fig. 2b one can see direct connection of CuO_2 planes across the "b" type boundary which is likely to favour a high J_c. Amorphous phases can also be observed in some regions of the "b" type boundary (often close to triple points). Partial edge dislocations are also observed by us and other workers [28] at such boundaries, so the "b" type boundary can have variable form. The "brick wall" and "railway switch" models offer a plausible description of the J_c performance of the $Bi_2Sr_2Ca_{n-1}Cu_nO_x$ system only if the structure of the "a" type low angle tilt boundary can support a high J_c. Furthermore the degree to which a high J_c is maintained as the grain boundary tilt angle is increased is of importance for the "railway switch" model.

A region of the "a" type boundary in Fig. 2a is shown at high magnification in Fig. 3 with the upper grain oriented at [110]. It has been shown [9] that the dots with strong dark contrast (indicated by arrows) represent columns of Bi atoms and other black dots with weaker contrast approximate the positions of Sr, Ca and Cu columns. As discussed in detail elsewhere [8,9], the boundary is both structurally and composi-

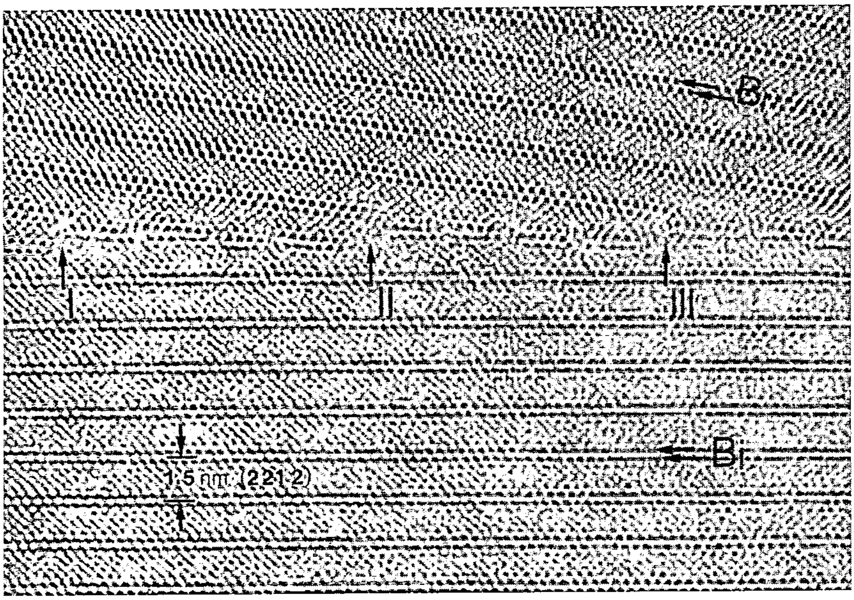

Fig. 3. A high magnification image in the typical areas of the low angle tilt boundary (marked by "a" in Fig. 2a). The (2201), (2212) and (2223) compounds can be seen locally at the boundary with the repeat distances for the modulated boundary structures.

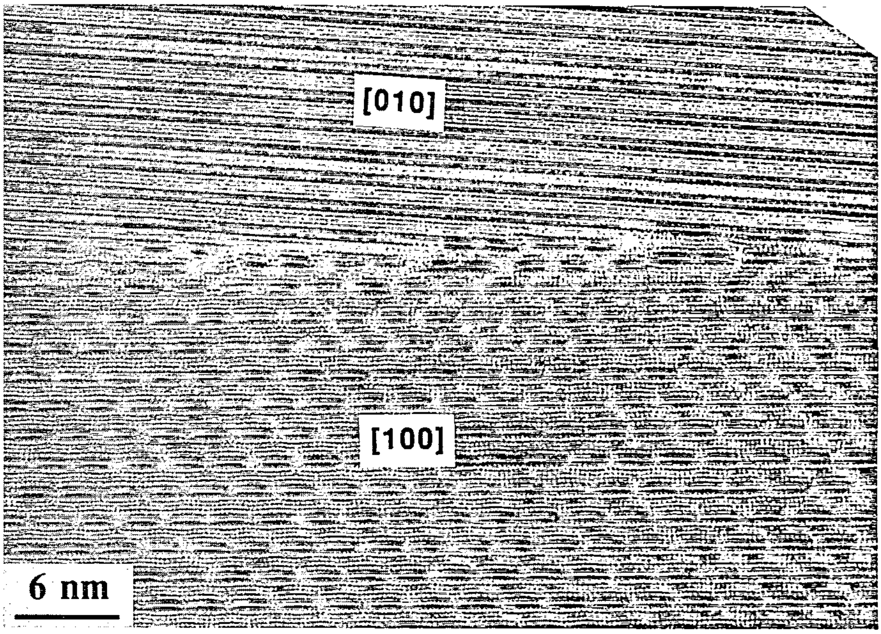

Fig. 4. An image of a region in which the habit plane of a low angle tilt boundary (marked IM) varies between the (001) planes of the two grains.

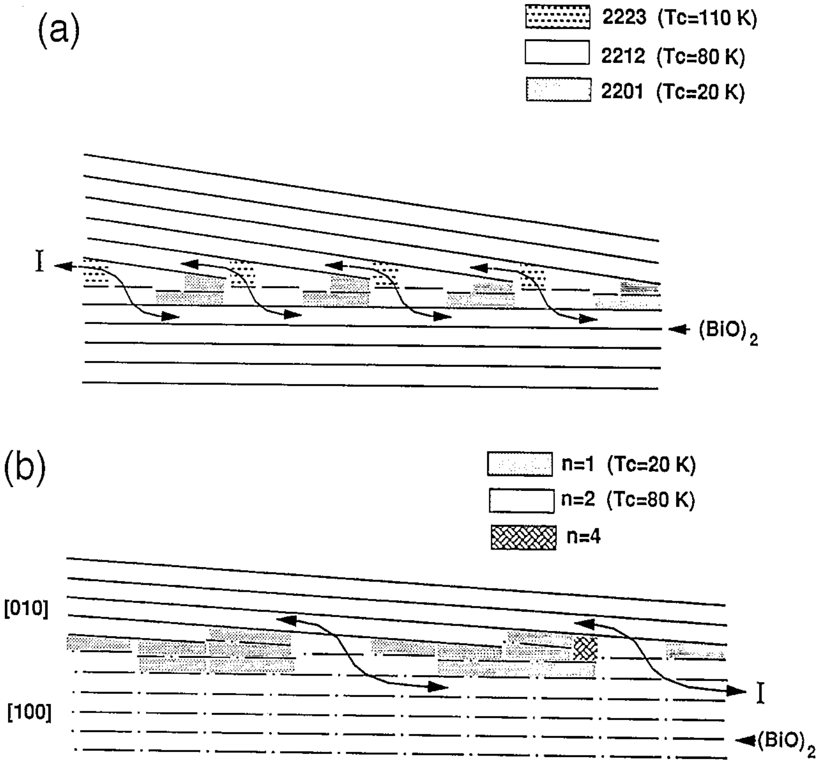

Fig. 5. A high magnification image of a 4° tilt boundary again associated with a near 90° twist about the c axis, now viewed along [0$\bar{1}$0] and [100] in the two respective grains.

tionally modulated using building blocks comprised of the compounds locally available to the parent phase by the incorporation or removal of CaO and CuO_2 layers. The structural changes along the boundary can be described using the notation $\{(n, n')/m\}$, in which n and n' denote the value of n (1, 2, 3...) for the $Bi_2Sr_2Ca_{n-1}Cu_nO_x$ phases locally present on each side of the boundary, while m denotes the number of $(a/2, b/2, 0)$ planes over which the given arrangement extends along the boundary in Fig. 3. In this way $\{(1, 2)/6\}$ would indicate the presence of a half unit cell height of the (2201) structure facing a half unit cell of the (2212) structure over six atomic columns (about 2.3 nm) in the ⟨110⟩ direction. The grain boundary structure repeats periodically, both between the arrows I and II and between II and III, by units of $\{(2, 3)/6\}$, $\{(2, 2)/7\}$, $\{(1, 2)/4\}$ and finally $\{(1, 1)/8\}$. Between the units there are slightly variable regions over which the BiO plane position is ill defined. This periodic repetition of the structure is necessarily associated with a periodic modulation of the local composition, although the fine scale of the modulation precludes accurate local compositional analysis using probe techniques. It is also notable that the relative distances along the boundary over which we see the (2223), (2212) and (2201) compounds (the values of m in the notation used here) differ. This reflects small differences in their relative formation energies and relates to the underlying mechanism for phase reconstruction at these low angle tilt boundaries [9]. The form of these boundaries differs markedly from that of similarly misoriented boundaries in the $YBa_2Cu_3O_{7-x}$ system, which provides an explanation for the good J_c performance in the $Bi_2Sr_2Ca_{n-1}Cu_nO_x$ system.

We have characterised boundaries at a variety of tilt angles and have found that, for tilts up to about 10°, composition modulation of the "a" type boundary described above is general. For boundaries of higher angle in the 0–10° range, intermediate habit planes were also observed (an example is shown in Fig. 4). The values of n and n' are normally less than three, while the values of m strongly depend on

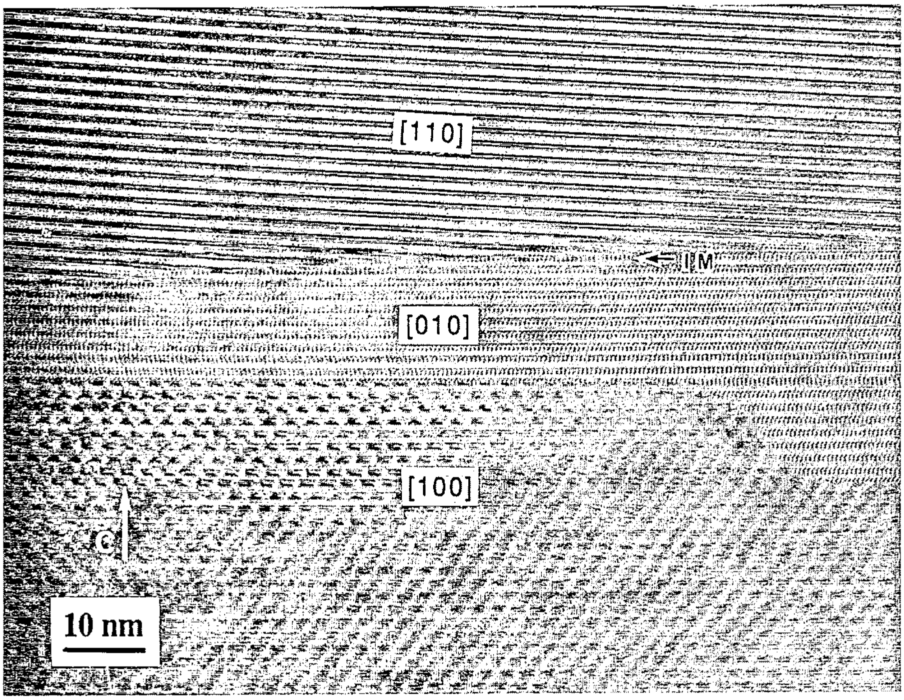

Fig. 6. Schematic diagrams of the low angle tilt boundaries shown in Figs. 3 and 5. High-T_c "pathways" crossing the boundary plane made up of the (2212) and (2223) phases can be seen. Supercurrents, as labelled, can flow between the grains on the a–b planes.

the tilt angle: the lower the tilt angle, the larger the values of m. Low angle tilt boundaries can simultaneously accommodate a twist angle approximating to 90° (see Fig. 5) or 45° (see Fig. 4). It is presumably similarities in the formation energies for the (2223), (2212) and (2201) compounds which both allow easy grain boundary relaxation for these low angle tilt boundaries and also lead to the common occurrence of this type of boundary. An image of a 4° tilt boundary which was also associated with a near 90° twist is shown in Fig. 5. The boundary area is viewed along the [100] direction in the lower grain while the orientation of the upper grain is within 2° of the [010] orientation (determined by selected area electron diffraction). We again see a periodic modulation of the boundary demonstrating that this is a general behaviour for low angle tilt boundaries in the $Bi_2Sr_2Ca_{n-1}Cu_nO_x$ system. The contrast associated with the incommensurate modulation of (2212) of the lower grain locally extends beyond the flat habit plane of the boundary by distances as large as the unit cell height. This suggests that the grain boundary structure shown in Fig. 5 is truly interwoven by the relaxation process, probably with important consequences for the J_c of such a boundary.

3. Orientation dependence of the critical current density of low angle tilt boundaries

The compositionally modulated boundaries described above are likely to favour a high J_c. Schematic diagrams of two typical low angle boundaries (as for 8° and 4° tilt) are shown in Figs. 6a and b indicating how local units of the (2201), (2212), and (2223) phases accommodate the gross mismatch. Although there are regions of the low-T_c (2201) phase ($T_c = 20$ K) at the boundary which are highly resistive at liquid nitrogen temperature, it is also clear that there are "pathways" crossing the boundary plane made up of the high-T_c (2212) and (2223) phases. High-T_c links of this general form were found to be present for the full range of tilt angles examined up to about 10°. These pathways are relatively wide and would, apart from reductions due to the strain associated with incomplete misfit relaxation, be expected to accommodate the full J_c of the high-T_c phases. Increasing misorientation leads to a reduction of the length of the local units and an increase in the locally retained strains. It is suggested that the remarkable structure of these boundaries is the origin of the high J_c seen in textured (2212) material at low temperatures. Furthermore, since such structures have not been found at grain boundaries in $YBa_2Cu_3O_{7-\delta}$, we also have a possible explanation for the differing effect of grain boundary orientation on the J_c value for the two materials.

In textured $Bi_2Sr_2CaCu_2O_x$ the supercurrent is relatively unimpeded at the actual grain boundary interface for low angle tilt boundaries. However because of the very short coherence length in the c direction, it is difficult to distribute the current beyond the boundary into the full cross-section of the neighbouring grain. The current in the c direction in (2212) single crystals has been shown to be a Josephson tunnel current and J_c is some two orders of magnitude less than the critical current density in the a–b plane [23]. Thus because of the limited critical current density in the c direction, the grains either need to be exceedingly thin so that current entering at the surface can readily spread in the c-direction across the whole grain cross-section, or alternatively the grains need to be very long so that there is the opportunity to gradually transfer the full critical current of the grain over a considerable length of grain boundary. We have noted above that the aspect ratio of grains for these materials is typically 10^2. Effective current spreading in the c direction is expected because the critical "a" type boundary structure extends to tilt angles of up to 10°.

The structure of high angle tilt (> 10°) boundaries in sintered $Bi_2Sr_2Ca_{n-1}Cu_nO_x$ samples has also been investigated by us [29]. The composition changes modulating the boundary structure only occur on one side of a high angle tilt (> 10°) boundary. The interfaces still tend to exhibit (001) plane facets, leaving steps of height equal to $c/2$ for the lower T_c phase with amorphous material at the corners of these steps. These observations suggest that a weak link is formed at high angle tilt boundaries where the whole boundary is blocked by amorphous materials and the (2201) phase. Amorphous materials are known to be non superconducting and the (2201) is only superconducting below about 20 K. It is therefore reasonable to suppose that, beside the crystallographic effect of high angle boundaries, these barriers lead to the low J_c in materials where a large proportion of boundaries have more than 10° misorientation [29].

4. Conclusions

A one-to-one correspondence between the critical current density and the structure for a given boundary can at present neither be theoretically modelled nor experimentally measured. However the structural models developed here for the low angle tilt boundaries in the $Bi_2Sr_2Ca_{n-1}Cu_nO_x$ system provide an explanation for the high J_c values observed for low texture breadths. In $Bi_2Sr_2Ca_{n-1}Cu_nO_x$ the current is not seriously limited by the low habit boundaries themselves but instead by the extreme anisotropy of the material and the difficulty of transporting the charge in the *c* direction after crossing the boundary. In contrast the anisotropy in $YBa_2Cu_3O_{7-\delta}$ is much less and the *c* axis critical current density is relatively high, the current across a grain boundary is limited by variable oxygen content [24] and any impurity phases [11–14] at the boundary. Like $Bi_2Sr_2Ca_{n-1}Cu_nO_x$ there are three related stable phases in the YBaCuO system: $Y_2Ba_4Cu_7O_x$(247), $YBa_2Cu_4O_x$(124), and $YBa_2Cu_3O_{7-\delta}$(123) with critical temperatures of about 40, 80, and 92 K respectively. The local (124) and (247) phases have often been found in the (123) phase. The similarities of the structures of these three phases [25–27] as well as the existence of the former two compounds in the (123) phase suggest that it may be possible to develop processing routes, involving controlled atmosphere annealing and appropriate doping additions, to encourage the incorporation of these compounds at grain boundaries in $YBa_2Cu_3O_{7-\delta}$ in a similar way to that described here for the BiSrCaCuO system. The characteristics of low angle tilt grain boundary structures we have described is not system limited. Indeed, since the lower the anisotropy of the superconductor the greater the increase in critical current density that will result from the incorporation of such "multiple phase structural boundaries", the improvements in J_c expected for $YBa_2Cu_3O_{7-\delta}$ are greater than for $Bi_2Sr_2CaCu_2O_x$.

References

[1] N. Uno, N. Enomoto, H. Kikuchi, K. Matsumoto, M. Mimura and M. Nakajima, Adv. Supercon. 2, Proc. Int. Symp. Supercon. 2nd (1991) p. 341.

[2] L.N. Bulaevskii, J.R. Clem, L.I. Glazman and A.P. Malozemoff, Phys. Rev. B 45 (1992) 2545.

[3] O. Eibl, Physica C 168 (1990) 239.

[4] O. Eibl, Physica C 168 (1990) 249.

[5] S. Horiuchi, K. Shoda, X.J. Wu, H. Nozaki and M. Tsutsumi, Physica C 168 (1990) 203.

[6] R. Ramesh, B.G. Bagley, J.M. Tarascon, S.M. Green, M.L. Rudee and H.L. Luo, J. Appl. Phys. 67 (1990) 379.

[7] B. Hensel, J.-C. Grivel, A. Jeremie, A. Perrin, A. Pollini and R. Flükiger, Physica C 205 (1993) 329.

[8] Y. Yan, J.E. Evetts, B. Soylu and W.M. Stobbs, Proc. of 13th Int. Congress on Electron Microscopy, Paris, Eds. B. Jouffrey and C. Colliex (Les Editions de Physiue Les Ulis, France) vol. 2 (July 1994) p. 967.

[9] Y. Yan, J.E. Evetts, B. Soylu and W.M. Stobbs, Philos. Mag. Lett. 70 (1994) 195.

[10] Y. Feng, K. Hautanen, Y.E. High, D.C. Larbalestier, R. Ray II, E.E. Hellstrom and S.E. Babcock, Physica C 192 (1992) 293.

[11] R.A. Camps, J.E. Evetts, B.A. Glowacki, S.B. Newcomb, R.E. Somekh and W.M. Stobbs, Nature 329 (1987) 229.

[12] S. Nakahara, G.J. Fisanick, M.F. Yan, R.B. Van Dover, T. Boone and R. Moore, J. Cryst. Growth 85 (1987) 639.

[13] S.E. Babcock and D.C. Larbalestier, Appl. Phys. Lett. 55 (1989) 393.

[14] S.E. Babcock, N. Zhang, Y. Gao, X.Y. Cai, D.L. Kaiser, D.C. Larbalestier and K. Merkle, J. Adv. Sci. (Japan) 4 (1992) 199.

[15] J. Akimitsu, A. Yamazaki, H. Sawa and H. Fujiki, Jpn. J. Appl. Phys. 26 (1987) L2080.

[16] H. Maeda, Y. Tanaka, M. Fukutomi and T. Asano, Jpn. J. Appl. Phys. 27 (1988) L209.

[17] C. Michel, M. Hervieu, M.M. Borel, A. Grandin, F. Deslandes, J. Provost and B. Raveau, Z. Phys. B 68 (1987) 421.

[18] B. Soylu, N. Adamopoulos, D.M. Glowacka and J.E. Evetts, Appl. Phys. Lett. 60 (1992) 3183.

[19] N. Adamopoulos and J.E. Evetts, IEEE Trans. Appl. Superconductivity 3 (1993) 1257.

[20] P. Chaudhari, J. Mannhart, D. Dimos, C.C. Tsuei, J. Chi, M.M. Oprysko and M. Scheuermann, Phys. Rev. Lett. 60 (1988) 1653.

[21] D. Dimos, P. Chaudhari and J. Mannhart, Phys. Rev. B 41 (1990) 4038.

[22] D.C. Larbalestier, S.E. Babcock, X.Y. Cai, M.B. Field, Y. Gao, N.F. Heinig, D.L. Kaiser, K. Merkle, L.K. Williams and N. Zhang, Physica C 185–189 (1991) 315.

[23] Y.I. Latyshev, and J.E. Nevelskaya, 7th Int. Workshop on Critical Currents in Superconductors, ed. H.W. Weker (World Scientific, Singapore, 1994) p. 284.

[24] Y. Zhu, Z.L. Wang and M. Suenaga, Philos. Mag. A 67 (1993) 11.

[25] P. Marsh, R.M. Fleming, M.L. Mandich, A.M. DeSantolo, J. Kwo, M. Hong and L.J. Martinez-Miranda, Nature 334 (1988) 141.

[26] P. Bordet, C. Chaillout, J. Chenavas, J.L. Hodeau, M. Marezio, J. Karpinski and E. Kaldis, Nature 334 (1988) 596.

[27] J.J. Capponi, C. Chaillout, A.W. Hewat, P. Lejay, M. Marezio, N. Nguyen, B. Raveau, J.L. Soubeyroux, J.L. Tholence and R. Tournier, Europhys. Lett. 3 (1987) 1301.

[28] H. Budin, O. Eibl, P. Pongratz and P. Skalicky, Physica C 207 (1993) 208.

[29] Y. Yan, W. Lo, J.E. Evetts, A.M. Campbell and W.M. Stobbs, Appl. Phys. Lett. 67 (1995) 2554.